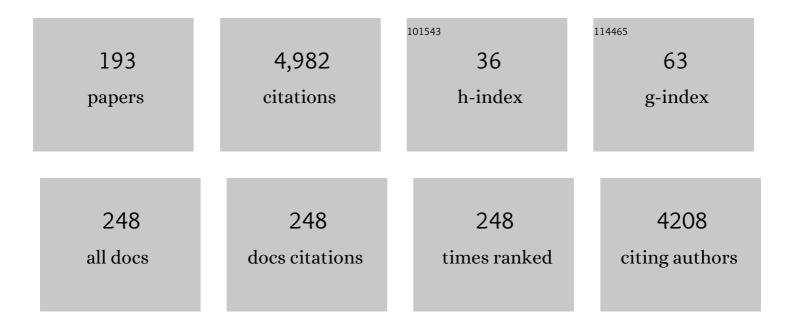
List of Publications by Year in descending order

Source: https://exaly.com/author-pdf/3535236/publications.pdf Version: 2024-02-01



#	Article	IF	CITATIONS
1	Endoscopic optical coherence tomography based on a microelectromechanical mirror. Optics Letters, 2001, 26, 1966.	3.3	279
2	A low-noise low-offset capacitive sensing amplifier for a 50-/spl mu/g//spl radic/Hz monolithic CMOS MEMS accelerometer. IEEE Journal of Solid-State Circuits, 2004, 39, 722-730.	5.4	262
3	Technologies for Cofabricating MEMS and Electronics. Proceedings of the IEEE, 2008, 96, 306-322.	21.3	209
4	Volatile Organic Compound Detection Using Nanostructured Copolymers. Nano Letters, 2006, 6, 1598-1602.	9.1	195
5	Laminated high-aspect-ratio microstructures in a conventional CMOS process. Sensors and Actuators A: Physical, 1996, 57, 103-110.	4.1	186
6	Inkjet printed chemical sensor array based on polythiophene conductive polymers. Sensors and Actuators B: Chemical, 2007, 123, 651-660.	7.8	177
7	Chronic tissue response to carboxymethyl cellulose based dissolvable insertion needle for ultra-small neural probes. Biomaterials, 2014, 35, 9255-9268.	11.4	170
8	Post-CMOS processing for high-aspect-ratio integrated silicon microstructures. Journal of Microelectromechanical Systems, 2002, 11, 93-101.	2.5	132
9	Micro-electro-mechanical systems (MEMS)-based micro-scale direct methanol fuel cell development. Energy, 2006, 31, 636-649.	8.8	129
10	A post-CMOS micromachined lateral accelerometer. Journal of Microelectromechanical Systems, 2002, 11, 188-195.	2.5	125
11	A Two-Axis Electrothermal Micromirror for Endoscopic Optical Coherence Tomography. IEEE Journal of Selected Topics in Quantum Electronics, 2004, 10, 636-642.	2.9	121
12	Micromachined high-Q inductors in a 0.18-μm copper interconnect low-k dielectric CMOS process. IEEE Journal of Solid-State Circuits, 2002, 37, 394-403.	5.4	110
13	Position Control of Parallel-Plate Microactuators for Probe-Based Data Storage. Journal of Microelectromechanical Systems, 2004, 13, 759-769.	2.5	102
14	Single-chip computers with microelectromechanical systems-based magnetic memory (invited). Journal of Applied Physics, 2000, 87, 6680-6685.	2.5	95
15	Electrostatically actuated resonant microcantilever beam in CMOS technology for the detection of chemical weapons. IEEE Sensors Journal, 2005, 5, 641-647.	4.7	92
16	Fabrication, characterization, and analysis of a DRIE CMOS-MEMS gyroscope. IEEE Sensors Journal, 2003, 3, 622-631.	4.7	89
17	A CMOS-MEMS mirror with curled-hinge comb drives. Journal of Microelectromechanical Systems, 2003, 12, 450-457.	2.5	89
18	A hierarchical circuit-level design methodology for microelectromechanical systems. IEEE Transactions on Circuits and Systems Part 2: Express Briefs, 1999, 46, 1309-1315.	2.2	85

#	Article	IF	CITATIONS
19	Vertical comb-finger capacitive actuation and sensing for CMOS-MEMS. Sensors and Actuators A: Physical, 2002, 95, 212-221.	4.1	84
20	Endoscopic optical coherence tomographic imaging with a CMOS-MEMS micromirror. Sensors and Actuators A: Physical, 2003, 103, 237-241.	4.1	83
21	Emerging simulation approaches for micromachined devices. IEEE Transactions on Computer-Aided Design of Integrated Circuits and Systems, 2000, 19, 1572-1589.	2.7	79
22	Integrated Microelectromechanical Gyroscopes. Journal of Aerospace Engineering, 2003, 16, 65-75.	1.4	79
23	Process technology for the modular integration of CMOS and polysilicon microstructures. Microsystem Technologies, 1994, 1, 30-41.	2.0	72
24	Endoscopic optical coherence tomography with a modified microelectromechanical systems mirror for detection of bladder cancers. Applied Optics, 2003, 42, 6422.	2.1	69
25	Paper generators. , 2013, , .		69
26	CMOS-MEMS Capacitive Humidity Sensor. Journal of Microelectromechanical Systems, 2010, 19, 183-191.	2.5	68
27	Design and modeling of a fluid-based micro-scale electrocaloric refrigeration system. International Journal of Heat and Mass Transfer, 2014, 72, 559-564.	4.8	68
28	Material Gradients in Stretchable Substrates toward Integrated Electronic Functionality. Advanced Materials, 2016, 28, 3584-3591.	21.0	52
29	Multimode digital control of a suspended polysilicon microstructure. Journal of Microelectromechanical Systems, 1996, 5, 283-297.	2.5	46
30	Estimation of line dimensions in 3D direct laser writing lithography. Journal of Micromechanics and Microengineering, 2016, 26, 105011.	2.6	46
31	CMOS–MEMS Lateral Electrothermal Actuators. Journal of Microelectromechanical Systems, 2008, 17, 103-114.	2.5	45
32	Stress Effects and Compensation of Bias Drift in a MEMS Vibratory-Rate Gyroscope. Journal of Microelectromechanical Systems, 2017, 26, 569-579.	2.5	44
33	Endoscopic optical coherence tomography with new MEMS mirror. Electronics Letters, 2003, 39, 1535.	1.0	43
34	An ultra-compliant, scalable neural probe with molded biodissolvable delivery vehicle. , 2012, , .		43
35	Ultra-miniature ultra-compliant neural probes with dissolvable delivery needles: design, fabrication and characterization. Biomedical Microdevices, 2016, 18, 97.	2.8	43
36	Ultracompliant Hydrogelâ€Based Neural Interfaces Fabricated by Aqueousâ€Phase Microtransfer Printing. Advanced Functional Materials, 2018, 28, 1801059.	14.9	43

#	Article	IF	CITATIONS
37	Electrostatic latching for inter-module adhesion, power transfer, and communication in modular robots. , 2007, , .		42
38	Robust gold nanoparticles stabilized by trithiol for application in chemiresistive sensors. Nanotechnology, 2010, 21, 405501.	2.6	42
39	Temperature stabilization of CMOS capacitive accelerometers. Journal of Micromechanics and Microengineering, 2004, 14, 559-566.	2.6	41
40	Optimization-based synthesis of microresonators. Sensors and Actuators A: Physical, 1998, 70, 118-127.	4.1	33
41	Resonant Microelectromechanical Receiver. Journal of Microelectromechanical Systems, 2019, 28, 327-343.	2.5	31
42	Hierarchical design and test of integrated microsystems. IEEE Design and Test of Computers, 1999, 16, 18-27.	1.0	30
43	Modeling and simulation of a condenser microphone. Sensors and Actuators A: Physical, 2008, 145-146, 224-230.	4.1	29
44	Electrocaloric characterization of a poly(vinylidene) Tj ETQq0 0 0 rgBT /Overlock 10 Tf 50 467 Td (fluoride-trifle Letters, 2014, 105, .	uoroethylen 3.3	e-chlorofluoro 27
45	CMOS-Based Sensors. , 0, , .		25
46	A quadratic-shaped-finger comb parametric resonator. Journal of Micromechanics and Microengineering, 2013, 23, 095007.	2.6	23
47	Hierarchical Mixed-Domain Circuit Simulation, Synthesis and Extraction Methodology for MEMS. Journal of Signal Processing Systems, 1999, 21, 233-249.	1.0	20
48	RF CMOS-MEMS capacitor having large tuning range. , 0, , .		20
49	CMOS-MEMS 3-bit Digital Capacitors With Tuning Ratios Greater Than 60:1. IEEE Transactions on Microwave Theory and Techniques, 2011, 59, 1238-1248.	4.6	20
50	In vitro electrochemical characterization of polydopamine melanin as a tissue stimulating electrode material. Journal of Materials Chemistry B, 2016, 4, 3031-3036.	5.8	20
51	Detection of free chloride in concrete by NMR. Cement and Concrete Research, 2004, 34, 379-390.	11.0	19
52	Design of a multi-axis implantable MEMS sensor for intraosseous bone stress monitoring. Journal of Micromechanics and Microengineering, 2009, 19, 085016.	2.6	19
53	CMOS-MEMS Variable Capacitors Using Electrothermal Actuation. Journal of Microelectromechanical Systems, 2010, 19, 1105-1115.	2.5	19
54	Large-displacement parametric resonance using a shaped comb drive. , 2013, , .		17

#	Article	IF	CITATIONS
55	Tri-axial high-g CMOS-MEMS capacitive accelerometer array. Proceedings of the IEEE International Conference on Micro Electro Mechanical Systems (MEMS), 2008, , .	0.0	16
56	Designing a robust high-speed CMOS-MEMS capacitive humidity sensor. Journal of Micromechanics and Microengineering, 2012, 22, 085021.	2.6	16
57	Interaction effects of temperature and stress on matched-mode gyroscope frequencies. , 2013, , .		16
58	The role of hierarchical design and morphology in the mechanical response of diatom-inspired structures <i>via</i> simulation. Biomaterials Science, 2018, 6, 146-153.	5.4	16
59	Interfacial delamination and delamination mechanism maps for 3D printed flexible electrical interconnects. Extreme Mechanics Letters, 2021, 43, 101199.	4.1	16
60	Schematic-based lumped parameterized behavioral modeling for suspended MEMS. IEEE/ACM International Conference on Computer-Aided Design, Digest of Technical Papers, 2002, , .	0.0	15
61	On-Chip High Quality Factor CMOS-MEMS Silicon-Fin Resonators. , 2007, , .		15
62	Simulation of stress effects on mode-matched MEMS gyroscope bias and scale factor. , 2014, , .		15
63	Writing nanometer-scale pits in sputtered carbon films using the scanning tunneling microscope. Applied Physics Letters, 1999, 74, 3902-3903.	3.3	14
64	Issues in MEMS macromodeling. , 0, , .		14
65	A 4-bit RF MEMS phase shifter monolithically integrated with conventional CMOS. , 2011, , .		12
66	Integrated vertical parallel-plate capacitive humidity sensor. Journal of Micromechanics and Microengineering, 2011, 21, 065028.	2.6	12
67	Behavioral Modeling of a CMOS–MEMS Nonlinear Parametric Resonator. Journal of Microelectromechanical Systems, 2013, 22, 1447-1457.	2.5	12
68	Gas chemical sensitivity of a CMOS MEMS cantilever functionalized via evaporation driven assembly. Journal of Micromechanics and Microengineering, 2014, 24, 075001.	2.6	11
69	Nonlinearity tuning and its effects on the performance of a MEMS gyroscope. , 2015, , .		11
70	Accelerometers. , 2008, , 135-180.		10
71	CMOS-MEMS variable capacitors with low parasitic capacitance for frequency-reconfigurable RF circuits. , 2009, , .		10
72	Dielectric charging effects in electrostatically actuated CMOS MEMS resonators. , 2010, , .		10

#	Article	IF	CITATIONS
73	Material Characterization and Transfer of Large-Area Ultra-Thin Polydimethylsiloxane Membranes. Journal of Microelectromechanical Systems, 2015, 24, 2170-2177.	2.5	10
74	Drop casting of stiffness gradients for chip integration into stretchable substrates. Journal of Micromechanics and Microengineering, 2017, 27, 045018.	2.6	10
75	High dynamic range CMOS-MEMS capacitive accelerometer array. , 2018, , .		10
76	Mechanical characterization of polydimethylsiloxane (PDMS) exposed to thermal histories up to 300 °C in a vacuum environment. Journal of Micromechanics and Microengineering, 2020, 30, 067001.	2.6	10
77	Multiphysics modeling of a micro-scale Stirling refrigeration system. International Journal of Thermal Sciences, 2013, 74, 44-52.	4.9	9
78	Design and Evaluation of a MEMS-Based Stirling Microcooler. Journal of Heat Transfer, 2013, 135, .	2.1	9
79	On-chip characterization of stress effects on gyroscope zero rate output and scale factor. , 2015, , .		9
80	Ultra-low-power and high sensitivity resonant micromechanical receiver. , 2017, , .		9
81	<title>Mechanical effects of fatigue and charge on CMOS MEMS</title> . , 2000, 4180, 108.		8
82	Picogram material dosing of microstructures. Journal of Applied Physics, 2009, 106, 104913.	2.5	8
83	On the origin of selectivity and anisotropy loss during microstructure release etch. Journal of Micromechanics and Microengineering, 2010, 20, 035021.	2.6	8
84	Application of statistical element selection to 3D integrated AlN MEMS filters for performance correction and yield enhancement. , 2015, , .		8
85	Sidewall Metallization on CMOS MEMS by Platinum ALD Patterning. Journal of Microelectromechanical Systems, 2020, 29, 978-983.	2.5	8
86	Hydrogel-based electrodes for selective cervical vagus nerve stimulation. Journal of Neural Engineering, 2021, 18, 055008.	3.5	8
87	MEMS-based endoscopic optical coherence tomography. , 2005, , .		7
88	BioImplantable Bone Stress Sensor. , 2005, 2006, 518-21.		7
89	CMOS-MEMS probes for reconfigurable IC's. Proceedings of the IEEE International Conference on Micro Electro Mechanical Systems (MEMS), 2008, , .	0.0	7
90	A Dual Probe STM Imaging System and a Low Noise Switched-Capacitor Transimpedance Amplifier. IEEE Sensors Journal, 2013, 13, 2984-2992.	4.7	7

#	Article	IF	CITATIONS
91	Bi-state control of parametric resonance. Applied Physics Letters, 2013, 103, 183512.	3.3	7
92	CMOS-MEMS resonant demodulator for near-zero-power RF wake-up receiver. , 2017, , .		7
93	A direct plasma etch approach to high aspect ratio polymer micromachining with applications in bioMEMS and CMOS-MEMS. , 0, , .		6
94	Polysilicon sensors for CMOS-MEMS electrothermal probes. , 2009, , .		6
95	Active CMOS-MEMS AFM-like conductive probes for field-emission assisted nano-scale fabrication. , 2010, , .		6
96	An ultra-low noise Switched Capacitor Transimpedance Amplifier for parallel Scanning Tunneling Microscopy. , 2012, , .		6
97	Effect of stress on matched-mode gyroscope frequencies. , 2014, , .		6
98	On-chip stress compensation on the ZRO of a mode-matched MEMS gyroscope. , 2016, , .		6
99	"Chip-size" antennas for implantable sensors and smart dust. , 0, , .		5
100	A CMOS MEMS Gold Plated Electrode Array for Chemical Vapor Detection. , 2006, , .		5
101	Polymer Mass Loading of CMOS/MEMS Microslot Cantilever for Gravimetric Sensing. , 2007, , .		5
102	An optimal design of high performance interface circuit with acoustic transducer model. , 2007, , .		5
103	CMOS-MEMS Filters. , 2008, , .		5
104	Enhancing CMOS Using Nanoelectronic Devices: A Perspective on Hybrid Integrated Systems. Proceedings of the IEEE, 2010, 98, 2061-2075.	21.3	5
105	Active CMOS-MEMS conductive probes and arrays for tunneling-based atomic-level surface imaging. , 2011, , .		5
106	The use of coated gold nanoparticles in high performance chemical sensors. , 2014, , 231-253.		5
107	<title>Characterization and reliability of CMOS microstructures</title> . , 1999, 3880, 132.		4
108	A MEMS-based monolithic electrostatic microactuator for ultra-low magnetic disk head fly height control. IEEE Transactions on Magnetics, 2001, 37, 1915-1918.	2.1	4

#	Article	IF	CITATIONS
109	Regioregular polythiophene nanowires and sensors. , 2005, , .		4
110	Modeling and Simulation of a Condenser Microphone. , 2007, , .		4
111	CMOS-MEMS Capacitive Humidity Sensor. , 2009, , .		4
112	Electrically driven CMOS-MEMS nonlinear parametric resonator design using a hierarchical MEMS circuit library. , 2011, , .		4
113	Statistical design and optimization for adaptive post-silicon tuning of MEMS filters. , 2012, , .		4
114	SI-CMOS-MEMS dual mass resonator for extracting mass and spring variations. , 2013, , .		4
115	Modulation of Parylene-C to silicon adhesion using HMDS priming. Journal of Micromechanics and Microengineering, 2014, 24, 105001.	2.6	4
116	Characterization of a CMOS sensing core for ultra-miniature wireless implantable temperature sensors with application to cryomedicine. Medical Engineering and Physics, 2014, 36, 1191-1196.	1.7	4
117	Hermetic Wafer Level Thin Film Packaging for MEMS. , 2016, , .		4
118	Processing of platinum electrodes for parylene-C based neural probes. , 2016, , .		4
119	A transfer process to fabricate ultra-compliant neural probes in dissolvable needles. Journal of Micromechanics and Microengineering, 2017, 27, 035008.	2.6	4
120	On-chip environmental sensors for bias drift compensation. , 2017, , .		4
121	A High Dynamic Range CMOS-MEMS Accelerometer Array with Drift Compensation and Fine-Grain Offset Compensation. , 2019, , .		4
122	Inkjet Printing of Curing Agent on Thin PDMS for Local Tailoring of Mechanical Properties. Macromolecular Rapid Communications, 2020, 41, 1900569.	3.9	4
123	Photolithographic Microfabrication. Handbook of Sensors and Actuators, 1998, , 13-61.	0.0	3
124	Phase and Vibration Analysis for a CMOS-MEMS Gyroscope. International Journal of Nonlinear Sciences and Numerical Simulation, 2002, 3, .	1.0	3
125	Polymer wicking to mass load cantilevers for chemical gravimetric sensors. , 0, , .		3

#	Article	IF	CITATIONS
127	RF-CMOS-MEMS based frequency-reconfigurable amplifiers. , 2009, , .		3
128	A CMOS-MEMS rotary microactuator suitable for hard disk drive applications. , 2009, , .		3
129	Lever-Based CMOS-MEMS Probes for Reconfigurable RF IC's. , 2009, , .		3
130	Model for aspect ratio dependent etch modulated processing. Journal of Vacuum Science and Technology A: Vacuum, Surfaces and Films, 2010, 28, 334-346.	2.1	3
131	Three-DOF CMOS-MEMS probes with embedded piezoresistive sensors. , 2010, , .		3
132	A SI-CMOS-MEMS process using back-side grinding. , 2010, , .		3
133	A Frenkel-Poole model of dielectric charging in CMOS MEMS. , 2011, , .		3
134	Behavioral modeling and testing of a CMOS-MEMS parametric resonator governed by the nonlinear Mathieu equation. , 2012, , .		3
135	Release and transfer of large-area ultra-thin PDMS. , 2014, , .		3
136	Tuning of nonlinearities and quality factor in a mode-matched gyroscope. , 2014, , .		3
137	Elastic ribbon-like piezoelectric energy harvester for wearable devices with stretchable surfaces. , 2016, 2016, 4816-4819.		3
138	Ultra-compliant peripheral nerve cuff electrode with hydrogel adhesion. , 2018, , .		3
139	Hourglass-beam Nanogram-proof-mass Array: Toward a High Dynamic Range Accelerometer. , 2019, , .		3
140	A Reconfigurable High-Bandwidth CMOS-MEMS Capacitive Accelerometer Array with High-g Measurement Capability and Low Bias Instability. , 2020, , .		3
141	Stress-and-Temperature-Induced Drift Compensation on a High Dynamic Range Accelerometer Array Using Deep Neural Networks. , 2021, , .		3
142	High onductivity Crackâ€Free 3D Electrical Interconnects Directly Printed on Soft PDMS Substrates. Advanced Materials Technologies, 2022, 7, .	5.8	3
143	<title>Design and simulation of thermal actuators for STM applications in a standard CMOS process</title> . , 1999, 3875, 32.		2
144	A two-axis electrothermal SCS micromirror for biomedical imaging. , 0, , .		2

#	Article	IF	CITATIONS
145	Volatile Organic Compound Discrimination Using Nanostructured Polythiophene Sensors. , 0, , .		2
146	Single-Crystal Silicon Based Electrothermal MEMS Mirrors for Biomedical Imaging Applications. , 2006, , 1429-1471.		2
147	Silicon Undercut Characterization in a CMOS-MEMS Process. , 2007, , .		2
148	A schematic-based design model for microphone and circuit integration. , 2007, , .		2
149	High current low contact resistance platinum-coated CMOS-MEMS probes. , 2010, , .		2
150	2-DoF twisting electrothermal actuator for Scanning Laser Rangefinder application. , 2011, , .		2
151	Ultra-compliant neural probes are subject to fluid forces during dissolution of polymer delivery vehicles. , 2013, 2013, 1550-3.		2
152	Bi-state control of a duffing microresonator on the falling edge of the instability. , 2013, , .		2
153	Design of a Fluid-Based Micro-Scale Electrocaloric Refrigeration System. , 2013, , .		2
154	Large stroke electrostatic actuated PDMS-on-silicon micro-pump. , 2015, , .		2
155	A silicon neural probe fabricated using DRIE on bonded thin silicon. , 2016, 2016, 4885-4888.		2
156	Self-healing narrowband filters via 3D heterogeneous integration of AlN MEMS and CMOS chips. , 2017, , .		2
157	Frequency Staggered Accelerometer Array for Improved Ringdown Behavior. , 2019, , .		2
158	ALD Titania Sidewalls on a CMOS-MEMS Resonator Oscillator and Effects on Resonant Frequency Drift. , 2019, , .		2
159	Compliant adhesive cuff electrode for selective stimulation in rat vagus nerve. , 2019, , .		2
160	Design of Direct Methanol Micro Fuel Cell Fluidic Systems. , 2002, , .		2
161	<title>Modeling methodology for a CMOS-MEMS electrostatic comb</title> . , 2002, 4755, 114.		1

#	Article	IF	CITATIONS
163	Accuracy and composability in NODAS. , 0, , .		1
164	Mechanisms of process-induced heating of MEMS structures during plasma release etch. , 2010, , .		1
165	Ultra-miniature wireless temperature sensor for thermal medicine applications. Proceedings of SPIE, 2011, 7901, .	0.8	1
166	Design and Evaluation of MEMS-Based Stirling Cycle Micro-Refrigeration System. , 2011, , .		1
167	Refined Si-CMOS-MEMS process using AOE, drie and preform bonding. , 2011, , .		1
168	Numerical Modeling of a Micro-Scale Stirling Cooler. , 2012, , .		1
169	A test structure to inform the effects of dielectric charging on CMOS MEMS inertial sensors. , 2012, , .		1
170	Ultra-low power frequency and duty-cycle modulated implantable pressure-temperature sensor. , 2013, , ,		1
171	Active CMOS-MEMS dual probe array for STM based parallel imaging and nanopatterning. , 2013, , .		1
172	Self-healing narrowband filters via 3D heterogeneous integration of AlN MEMS and CMOS chips. , 2017, , .		1
173	Insulation of thin-film parylene-C/platinum probes in saline solution through encapsulation in multilayer ALD ceramic films. Biomedical Microdevices, 2018, 20, 61.	2.8	1
174	Residual voltage as an ad-hoc indicator of electrode damage in biphasic electrical stimulation. Journal of Neural Engineering, 2021, 18, 0460c1.	3.5	1
175	System-Level Simulation of Microsystems. , 2006, , 187-227.		1
176	System-Level Simulation of Microsystems. , 2006, , 187-227.		1
177	Thermo-Fluids Considerations in the Development of a Silicon-based Micro-scale Direct Methanol Fuel Cell. , 2004, , .		1
178	Endoscopic optical coherence tomography with a micromachined mirror. , 0, , .		0
179	Silicon-Based Microdialysis Chip with Integrated Fraction Collection. , 0, , .		0
180	The Effect of a Distributed Mass Loading on the Frequency Response of a MEMS Mesh Resonator. , 2006, 2006, 1862-5.		0

#	Article	IF	CITATIONS
181	Platinum sputtered CMOS-MEMS electrothermal probes with piezoresistive force sensing. , 2009, , .		0
182	Aspect ratio dependent etch modulation for CMOS-MEMS applications. , 2009, , .		0
183	Scaling of folded electrothermal actuators. , 2010, , .		0
184	Self-engaging and disengaging CMOS-MEMS probes. , 2011, , .		0
185	(Invited) CMOS MEMS Integration. ECS Transactions, 2011, 35, 331-340.	0.5	0
186	A high-speed, bimodal, CMOS-MEMS resonant scanner driven by temperature-gradient actuators. Proceedings of SPIE, 2012, , .	0.8	0
187	Bi-State Bifurcation Control of a Shaped-Comb Parametric Resonator. , 2013, , .		0
188	A tunable notch filter using high-k <inf>t</inf> ² lithium niobate resonators toward integration in filter banks. , 2015, , .		0
189	Engineered Material Gradients for Biologically Integrated Stretchable Electronics. Biophysical Journal, 2015, 108, 331a.	0.5	0
190	Reconfigurable AlN resonator filter design based on extended statistical element selection. , 2017, , .		0
191	In Memoriam Harvey C. Nathanson 1936–2019. Journal of Microelectromechanical Systems, 2020, 29, 2-2.	2.5	0
192	Lateral Flexure Contact on CMOS MEMS Electrothermal Metal-Metal Contact Switch by Platinum ALD Sidewall Patterning. , 2021, , .		0
193	Aerosol-Jet-Printed Stretchable Electronic Decal Technology. , 2022, , .		0